

PDF hosted at the Radboud Repository of the Radboud University Nijmegen

The following full text is a publisher's version.

For additional information about this publication click this link.

<http://hdl.handle.net/2066/35354>

Please be advised that this information was generated on 2021-09-20 and may be subject to change.

Spectral Function of Ferromagnetic 3d Metals: A Self-Consistent LSDA + DMFT Approach Combined with the One-Step Model of Photoemission

J. Braun, J. Minár, and H. Ebert

Department Chemie und Biochemie, Physikalische Chemie, Ludwig-Maximilians Universität München, D-81377 München, Germany

M. I. Katsnelson¹ and A. I. Lichtenstein²

¹*University of Nijmegen, NL-6525 ED Nijmegen, The Netherlands*

²*Institut für Theoretische Physik, Universität Hamburg, D-20355 Hamburg, Germany*

(Received 2 August 2006; published 1 December 2006)

The electronic structure of ferromagnetic 3d-transition metals in the vicinity of the Fermi level is dominated by the spin-polarized *d* bands. Experimentally, this energy region can be probed in detail by means of angle-resolved ultraviolet photoemission and inverse photoemission. In several earlier studies the measured spectra were described either within a single-particle approach based on the local spin-density approximation including matrix-element effects within the so-called one-step model or by sophisticated many-body approaches neglecting these effects. In our analysis we combine for the first time correlation with matrix-element effects to achieve an improved interpretation of photoemission data from ferromagnetic nickel.

DOI: [10.1103/PhysRevLett.97.227601](https://doi.org/10.1103/PhysRevLett.97.227601)

PACS numbers: 79.60.Bm, 71.15.Mb, 73.20.-r, 75.70.Rf

The interest in magnetic materials and their surfaces has grown enormously over the last few decades. Especially the technological relevance of low-dimensional magnetic structures has triggered a lot of research activity. In this context a quantitative controlling of the magnetic properties is of essential importance. Moreover, material design on the nanometer scale is intimately connected with a detailed understanding of the electronic and magnetic structure of the corresponding solid surface. From the experimental point of view, the interesting valence-band region around the Fermi energy is probed in a most detailed and reliable way by ultraviolet photoemission spectroscopy (PES) [1] and inverse photoemission spectroscopy (IPE) [2]. Modern experimental arrangements supply not only spin resolution but also extremely high angle and energy resolution and in consequence reveal details of the spin-dependent band structure within some meV [3]. To keep up with the experimental progress an improved description of electronic correlation is strongly demanded, of course in combination with a realistic calculation of excitation spectra. In other words, the spectral function has to be determined including correlation effects for a semi-infinite solid and moreover the photoemission matrix elements have to be included in an appropriate way on the same footing.

In our approach the electronic structure is described within the framework of the fully relativistic Korringa-Kohn-Rostoker multiple-scattering theory (SPRKKR) [4]. To account properly for electronic correlations beyond the local spin-density approximation (LSDA) [5,6] we have introduced a general nonlocal, site-diagonal, complex, and energy-dependent self-energy Σ_{DMFT} [7], which is included self-consistently in the SPRKKR formalism and determined by a self-consistent dynamical mean field theory (DMFT) calculation for an ordered system with trans-

lational invariance. The LSDA + DMFT method is straightforwardly applicable to semi-infinite lattices with perfect lateral translational invariance and arbitrary number of atoms per unit cell. This has been recently demonstrated for angle-integrated valence-band photoemission [8].

The electronic structure calculation described above serves as a quantitative tool in determining the bare spectral function but certainly does not account for surface- and matrix-element effects visible in the measured intensity distributions. To achieve a reliable interpretation of the experimental spectra, it is therefore inevitable to deal quantitatively with the following points. First of all, the wave-vector and energy dependence of the transition-matrix elements have to be accounted for. These dependencies are known to be quite pronounced and therefore cannot be neglected. They result from strong multiple-scattering processes in the initial as well as in the final state which dominate the electron dynamics in the low-energy regime of typically 1–200 eV [9]. The transition-matrix elements also include the effects of selection rules. Last but not least, a realistic description of the surface barrier is essential for a quantitative description of surface states and resonances in simple metals like Ni [10,11], but also in more complex structures like thin films and multilayers.

The most successful theoretical approach to PES/IPE is the so-called one-step model of photoemission as originally proposed by Pendry and co-workers [9,12,13]. A review on the recent developments and refinements [14] of the approach can be found in [15,16]. The main idea of the one-step model is to describe the actual excitation process, the transport of the photoelectron to the crystal surface as well as the escape into the vacuum [17] as a single quantum-mechanically coherent process including

all multiple-scattering events. Therefore, the coupling of the bare spectral function corresponding to the LSDA potentials and the additional self-energy Σ_{DMFT} with the photoemission matrix elements is treated on the same footing on a very fundamental level.

In particular, the inclusion of dynamical correlation effects in 3d-transition metals like Ni is treated within the recently proposed fully (charge and self-energy) self-consistent LSDA + DMFT scheme [4]. Within the relativistic extension of this approach, correlation effects are represented by a complex self-energy Σ_{DMFT} that enters the Dirac-Hamiltonian that in turn is used to calculate the Green's function $G(E)$ by means of the multiple-scattering formalism. The correlation effects are treated here in the framework of DMFT [7], with a spin-polarized T -matrix fluctuation exchange (SPTF) type of DMFT solver [18]. Since the average electron-electron interactions are included already in the LSDA “double counting” (DC) terms have to be taken into account.

The LSDA exchange-correlation potential is an orbital averaged quantity and it turns out from the comparison of theoretical photoemission data (see below) with experiment, that we have to use the following form for the DC term: $\Sigma_{l,m_i,\sigma}(E) = \Sigma_{l,m_i,\sigma}(E) - \langle \Sigma_{l,m_i,\sigma}(E_f) \rangle$, e.g., for a given spin σ the average over d orbitals ($l = 2$). In particular, this DC results in a nonzero self-energy at the Fermi level. This properly describes the spectroscopic properties close to the Fermi level [19], but does not change the ground state properties calculated by LSDA + DMFT (for example, the spin magnetic moment). The self-consistent LSDA + DMFT calculations were carried out for the experimental ground state crystal structure, i.e., fcc-Ni. The lattice parameter was fixed at the experimental bulk value (6.658 a.u.). For parametrization of the corresponding LSDA exchange and correlation potential the results of Vosko *et al.* [20] were used. SCF convergence was achieved using 1639 k points within the irreducible Brillouin zone. The self-energy within the DMFT has been applied only for d states and can be calculated in terms of two parameters—the averaged screened Coulomb interaction U and the exchange interaction J . The screening of the exchange interaction is usually small and the value of J can be calculated directly and is approximately equal to 0.9 eV for all 3d elements. This value has been adopted for all of our calculations presented here. For U we used a value of 3 eV. However, our test calculations show that the choice of U does not substantially change features and trends in the calculated spectra.

The imaginary part $\text{Im}\Sigma_{\text{DMFT}}$ of the self-energy, that represents damping processes in the quasiparticle spectrum, is properly included in both the initial and the final states. This, for example, allows for transitions into evanescent band gap states decaying exponentially into the solid. Similarly, the assumption of a finite lifetime for the initial states gives access to photoemission intensities from

surface states and resonances. Treating the initial and final states within the fully relativistic version of the low-energy electron diffraction (LEED) theory [9], it remains a straightforward task to design complex layered structures like thin films and multilayers within the photoemission theory. First we apply our method to electronic structure and spin-resolved photoemission calculations of ferromagnetic Ni(001). We start the discussion with the electronic structure of Ni(001). Figure 1 shows the spin-polarized band structure in the occupied regime plotted along the Δ direction. Because of the simultaneous occurrence of spin-orbit coupling and exchange splitting which is treated on equal footing in a fully relativistic theory, majority and minority bands occur together for regions where the spin character is no longer well defined due to hybridization. For that reason we do not explicitly distinguish between majority and minority states as it is usual in nonrelativistic band structure calculations. The black color indicates the result of a conventional DFT calculation applying the LSDA, whereas the orange (light) colored bands illustrate the LSDA + DMFT calculation for which the imaginary part of the self-energy Σ_{DMFT} has been suppressed. The deviations between both band structures are clearly observable. The bands resulting from the LSDA + DMFT calculation are shifted towards the Fermi level compared with the pure LSDA-derived bands leading to a reduction

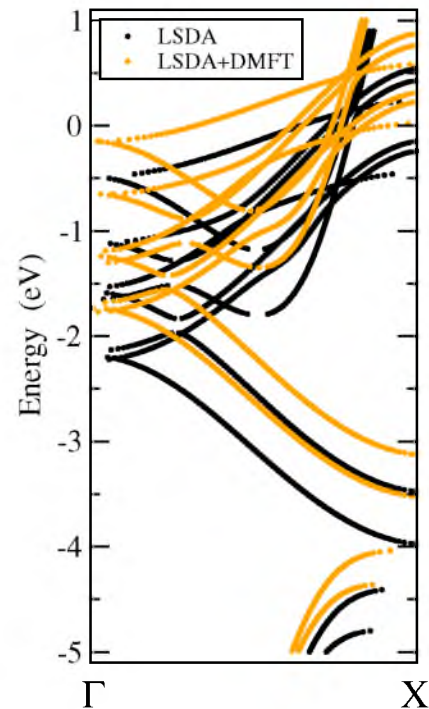


FIG. 1 (color online). Fully relativistic valence-band states of Ni(001) along ΓX . Black color indicates the LSDA-based calculation; orange (light) color denotes the states derived by the LSDA + DMFT method obtained by suppressing the imaginary part of Σ_{DMFT} .

of the d -band width. Also, the dispersion behavior is different and the spin splitting is significantly reduced. All of these effects have to be assigned to the real part of the self-energy Σ_{DMFT} that acts as a nonlocal, site-diagonal, spin- and energy-dependent potential on the various d bands of Ni.

In Fig. 2 we present a series of angle-resolved ultraviolet photoemission (ARUPS) spectra for different emission angles along the ΓLUX direction of the Ni(001) surface Brillouin zone. For normal emission a relatively sharp double-peak structure is visible 0.1 eV below the Fermi level in the spin-integrated spectrum. The peak structure is bulklike with a significant admixture of surface-state emission [10] because ultraviolet photoemission is in general sensitive to the surface band structure. With spin resolution it becomes clear that the peak with lower binding energy belongs to the minority-spin channel, whereas the second peak with lower intensity is identified as emission from majority-spin states. The effective spin splitting is 0.2 eV. Going to higher angles of emission the intensity distributions in both spin channels get broadened and the single spectral features evolve to multiple peak structures that

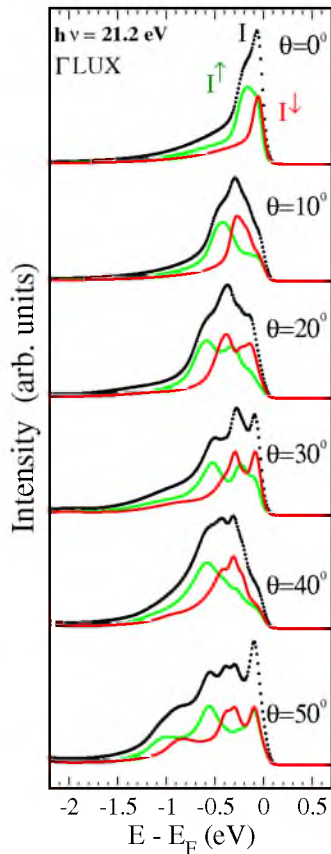


FIG. 2 (color online). ARUPS spectra from the Ni(001) surface Brillouin zone in the ΓX direction calculated for $h\nu = 21.2$ eV excitation energy. Black color indicates the spin-integrated intensities; green (light) color denotes the majority-spin channel; red (dark) color indicates minority-spin emission.

arise from excitation of various Ni d bands in combination with surface-state emission. The explanation is simply found in the dipole selection rules which allows more direct transitions in the off-normal case because of the reduced symmetry. This phenomenon is well known in angle-resolved photoemission and may be identified as a typical matrix-element effect generally neglected in standard many-body investigations.

A comparison of our results for Ni(011) with a former theoretical study and the corresponding experimental spectra [21] is presented in Fig. 3. In the upper row spin-integrated ARUPS measurements from Ni(011) along $\Gamma\bar{Y}$ for different angles of emission are shown. The dotted lines represent the experimental data, whereas the solid lines denote the single-particle approach to the measured spectral function. Obviously, the LSDA-based calculation completely fails. The energetic positions of the theoretical peaks deviate strongly from the measured ones. Furthermore, the complicated intensity distributions that appear for higher angles of emission could not be reproduced by the LSDA method at all. In contrast, the non-self-consistent quasiparticle calculation provides a significant improvement when compared to the measured spectra. For the complete variety of emission angles the energetic peak positions coincide with the experiment within about 0.1 eV.

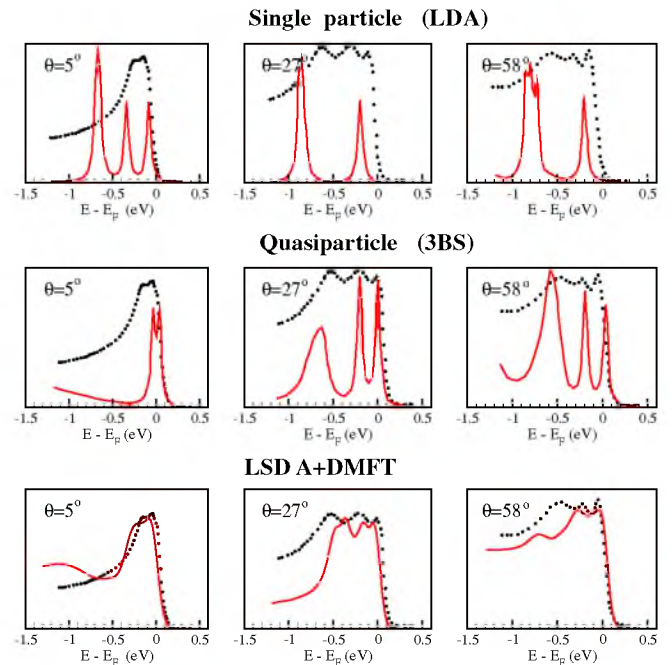


FIG. 3 (color online). Spin-integrated ARUPS spectra from Ni(011) along $\Gamma\bar{Y}$ for three different angles of emission. Upper row: comparison between LSDA-based calculation and experiment [21], middle row: comparison between experiment and non-self-consistent quasiparticle calculations neglecting matrix element and surface effects [21], lower row: spin-integrated LSDA + DMFT spectra including photoemission matrix elements (this work). Theory: solid red line, experiment: black dots.

Only the overall shape of the measured spectral intensities deviate from the calculations because of the neglect of multiple scattering and surface-related effects. In the experiment the different peaks seem to be more broadened and the spectral weight especially for nearly normal emission is shifted by about 0.1 eV to higher binding energies. In addition, it seems that for very high emission angles like 60° an even more complicated peak structure is hidden in the experimental resolution. An additional spin analysis is therefore highly desirable for these experiments.

Within our work we could go far beyond previous theoretical studies by combining a sophisticated many-body approach like the self-consistent LSDA + DMFT method with a so-called one-step based calculation of the corresponding spectral function. The resulting intensity distributions are shown in the lower row of Fig. 3. A first inspection reveals very satisfying quantitative agreement between experiment and theory for all emission angles. Let us concentrate first on the excitation spectrum calculated for $\Theta = 5^\circ$. The spin-integrated spectrum exhibits a pronounced double-peak structure with binding energies of 0.1 eV and 0.3 eV. The second peak is slightly reduced in intensity which is also in accordance with the experimental findings. Furthermore, the width of the spectral distribution is quantitatively reproduced. The calculated binding energies can be ascribed to the real part of the self-energy that corrects the peak positions due to dynamical renormalization procedure of the quasiparticles which is missing in a typical LSDA-based calculation. The relative intensities and the widths of the different peaks, on the other hand, must be attributed to the matrix-element effects which enter our calculations from the very beginning via the one-step model of photoemission. As it has been found for Ni(001) the double-peak structure originates from excitation of the spin-split d bands in combination with a significant amount of surface-state emission [11]. The two spectra calculated for high angles of emission show the more broadened spectral distributions observable from the experimental data. An explanation can be given in terms of matrix-element effects, due to the dominating dipole selection rules. The spin-resolved spectra reveal a variety of d -band excitations in both spin channels, which in consequence lead to the complicated shape of the spectral distributions hardly to be interpreted in the spin-integrated mode.

In conclusion, we have presented for the first time spectral function calculations of ferromagnetic Ni, which closely combine an improved description of electronic correlations with multiple-scattering, surface emission, dipole selection rules and other matrix-element related effects that lead to a modification of the relative peak intensities. As has been demonstrated, this approach allows on the one hand a detailed and reliable interpretation of high-resolution angle-resolved photoemission spectra of $3d$ ferromagnets. On the other hand, it also allows for a

very stringent test of new developments in the field of DMFT and similar many-body techniques.

Financial support from the Deutsche Forschungsgemeinschaft is gratefully acknowledged.

-
- [1] *Photoemission and the Electronic Properties of Surfaces*, edited by B. Feuerbacher, B. Fitton, and R.F. Willis (Wiley, New York, 1978); *Photoemission in Solids*, edited by M. Cardona and L. Ley (Springer, New York, 1978), Vol. 1; J.E. Inglesfield, Rep. Prog. Phys. **45**, 223 (1982); R. Courths and S. Hüfner, Phys. Rep. **112**, 53 (1984); *Angle-Resolved Photoemission, Theory, and Current Applications Studies in Surface Science and Catalysis*, edited by S.D. Kevan (Elsevier, Amsterdam, 1992), Vol. 74.
 - [2] V. Dose, Prog. Surf. Sci. **13**, 225 (1983); Surf. Sci. Rep. **5**, 337 (1985); G. Borstel and G. Thörner, Surf. Sci. Rep. **8**, 1 (1988); N.V. Smith, Rep. Prog. Phys. **51**, 1227 (1988); M. Donath, Surf. Sci. Rep. **20**, 251 (1994).
 - [3] M. Mulazzi *et al.*, Phys. Rev. B **74**, 035118 (2006).
 - [4] J. Minár *et al.*, Phys. Rev. B **72**, 045125 (2005).
 - [5] P. Hohenberg and W. Kohn, Phys. Rev. **136**, B864 (1964); W. Kohn and L.J. Sham, Phys. Rev. **140**, A1133 (1965); L.J. Sham and W. Kohn, Phys. Rev. **145**, 561 (1966).
 - [6] R. O. Jones and O. Gunnarsson, Rev. Mod. Phys. **61**, 689 (1989).
 - [7] G. Kotliar and D. Vollhardt, Phys. Today **57**, No. 3, 53 (2004); A. Georges *et al.*, Rev. Mod. Phys. **68**, 13 (1996).
 - [8] J. Minár *et al.*, Phys. Rev. Lett. **95**, 166401 (2005).
 - [9] J. B. Pendry, *Low Energy Electron Diffraction* (Academic, New York, 1974).
 - [10] E. W. Plummer and W. Eberhardt, Phys. Rev. B **20**, 1444 (1979).
 - [11] W. Eberhardt *et al.*, Phys. Rev. Lett. **45**, 273 (1980).
 - [12] J. B. Pendry, Surf. Sci. **57**, 679 (1976).
 - [13] J. F. L. Hopkinson, J. B. Pendry, and D. J. Titterton, Comput. Phys. Commun. **19**, 69 (1980).
 - [14] B. Ginatempo, P. J. Durham, and B. I. Gyorffy, J. Phys.: Condens. Matter **1**, 6483 (1989); S. V. Halilov *et al.*, J. Phys.: Condens. Matter **5**, 3859 (1993); J. Henk *et al.*, Phys. Rev. B **50**, 8130 (1994); M. Fluchtmann *et al.*, Phys. Rev. B **52**, 9564 (1995).
 - [15] J. Braun, Rep. Prog. Phys. **59**, 1267 (1996).
 - [16] J. Braun and M. Donath, J. Phys.: Condens. Matter **16**, S2539 (2004).
 - [17] C. N. Berglund and W. E. Spicer, Phys. Rev. **136**, A1030 (1964).
 - [18] M. I. Katsnelson and A. I. Lichtenstein, Eur. Phys. J. B **30**, 9 (2002).
 - [19] In particular, the long-standing problem of the Fermi surface of Ni, e.g., the hole pocket close to the X -symmetry point, was recently addressed within LSDA + DMFT method presented here. J. Minár *et al.*, Phys. Rev. B (to be published).
 - [20] S. H. Vosko, L. Wilk, and N. Nusair, Can. J. Phys. **58**, 1200 (1980).
 - [21] F. Manghi *et al.*, Phys. Rev. B **59**, R10409 (1999).